Diamond & Related Materials xxx (2009) xxx–xxx

Contents lists available at ScienceDirect

Diamond & Related Materials

journal homepage: www.elsevier.com/locate/diamond

Aligned diamond nano-wires: Fabrication and characterisation for advanced applications in bio- and electrochemistry

W. Smirnov *, A. Kriele, N. Yang, C.E. Nebel

Fraunhofer Institut für Angewandte Festkörperphysik, Tullastrasse 72, Freiburg 79108, Germany

ARTICLE INFO

Available online xxxx

Keywords:
Vertically aligned diamond nano-wires
Reactive ion etching
Electrochemistry
Electrodes
Biosensors

ABSTRACT

Nano-wires have become promising tools in a vast field of applications. Due to the many unique properties of diamond, the use of diamond nano-wires in biosensors attracts increasing attention. In this paper we introduce the realisation of wires from diamond using self-aligned nickel nano-particles as etching mask in an oxygen ICP dry etching step. With this process it is possible to create wires of high aspect ratios of 50, with diameters as small as 20 nm, and typical lengths of up to 1 μm on a large area in a dense pattern of about $10^{11}\,cm^{-2}$. The Ni nano-particles are formed by thermal annealing at 700 °C for 5 min of a thin (1 nm) Ni film that is deposited onto the diamond surface. The surface enhancement factor due to wires is dependent on the geometrical details of wires and was measured to be 10 to 80. The electrochemical properties of wires have been characterized by cyclic voltammetry using $Fe(CN)_6^{-3/-4}$ which shows that such topographies act as filter for redox molecules.

1. Introduction

Nano-wires are new and very promising materials for chemical and bio-chemical sensing since their geometrical properties can be tuned to match those of biological and chemical species. With dimensions in the nano-meter scale the electronic properties can be adjusted by low-dimensional effects. This can change the properties from those of bulk materials. One of the most striking aspects is the possibility to dramatically increase the surface-to-volume ratio of a given material.

Nano-wires from Si [1,2], SiO_2, InP [3], gold [4], SnO_2 [5] and nitride materials [6–8] have attracted much interest recently. Bottom–up as well as top–down approaches have been used to generate such nano-structures, which open up many new applications. However, wires from these materials do not fulfil the necessary chemical stability, hardness and bio-compatibility requirements. Sensors from these materials for example will suffer from corrosion and will degrade their functionality in harsh environments. In the past, the vast majority of research concentrated on carbon nano-tubes (CNTs) [9,10] which show outstanding mechanical [11] and electrical properties and which is therefore one of the most promising candidates for bio-applications. The other outstanding material is Diamond as it shows unique properties such as chemical stability and hardness [12] bio-compatibility and can be bio-functionalised with a variety of methods. The conductivity can be adjusted from insulating to semiconducting up to metallic by doping with boron. The surface can be terminated with oxygen or hydrogen which affects the wettability from hydrophilic to hydrophobic, resp. [13] and allows the electronic properties of the solid/electrolyte interface to be tuned with respect to energies of molecular layers. Electrodes from diamond have already shown superior properties compared to standard electrodes from graphite, Au or Pt with respect to low background current and wide electrochemical potential window [14]. Combining these advantages with features arising from nano-structured surfaces will yield a new generation of biosensors. Diamond nano-wires have already been fabricated [15] and used for chemical and bio-chemical sensing [16,17], mechanical reinforcement [18] and enhancements in thermal management [19]. Other promising applications of diamond nano-wires are for microelectronics and electron field emission devices [20–22] where the negative electron affinity is utilized [23].

Mostly two ways are used for fabrication of nano-wires namely bottom–up and top–down approaches. Diamond nano-wires were produced by overgrowing diamond homoepitaxially [24,25] or coating other materials like Si or carbon nano-tubes [26] with nano-diamond. The most often applied technique is a top–down approach, where diamond is etched with reactive ions in a plasma. Masking materials such as Al, SiO_2, Au, Ni and Mo can be deposited with help of lithographic techniques [27,28] on the diamond surface to protect selected areas from etching. Another approach uses unintentionally sputtered material from the substrate holder onto the sample during the etching process [28] or deliberately depositing thin metal layers, that will act as masking materials [29,30].

A low cost, fast, effective and reproducible method for the preparation of etching masks is the utilization of self-organised and self-assembling nano-particles from Al, Ni, Au [31,32], polymers, oxides,

* Corresponding author. Tel.: +49 761 5159 338.
E-mail address: Waldemar.Smirnov@iaf.fraunhofer.de (W. Smirnov).

0925-9635/$ – see front matter © 2009 Elsevier B.V. All rights reserved.
doi:10.1016/j.diamond.2009.09.001

nitrides and diamond powder [17]. Most of these techniques result in nano-wires which show low aspect ratios of height to width of typically 1:1 to 1:10 and densities which are in the range of $10^{10}\,cm^{-2}$.

In the present work we introduce and discuss the realisation of vertically aligned diamond nano-wires which show high aspect ratios, homogeneous and reproducible dimensions as well as controlled lengths. This is achieved by using self assembled Ni nano-particles which are used as etching mask in an inductively coupled plasma etching process (ICP). Resulting surface morphologies are investigated in detail using atomic force (AFM) and scanning electron microscopy (SEM). Electrochemical techniques have been applied to characterize surface enhancements and chemical activity of nano-wires.

2. Experimental

2.1. Diamond growth and substrate pretreatment

Undoped and heavily boron doped polycrystalline diamond films were grown in ellipsoidal shaped microwave plasma enhanced chemical vapour deposition (MWCVD) systems [33]. Substrates for diamond deposition were 3 in. silicon wafers. Process parameters were as following: a gas mixture of 3% methane in hydrogen, a microwave power of 3000 W and a total gas pressure of 100 mbar. The substrate temperature was held constant at 900 °C during deposition. To grow thick layers up to 300 h growth have been used at a deposition rate of $1\,\mu m\,h^{-1}$. To realize heavily boron doped films, boron concentrations of 1000 ppm were introduced into the gas phase. Boron doping levels were analysed by SIMS and capacitance-voltage (CV) [34] measurements and show doping levels of about $10^{21}\,cm^{-3}$. After growth, diamond surfaces were mechanically polished and silicon substrates were removed in a hot KOH bath. Segmenting of freestanding diamond wafers into (6×6) mm samples was performed with a Nd:YAG laser. Then the diamond samples were cleaned in chromium sulphuric acid, washed in deionised water (DI) and rinsed in a 1:1 mixture of HF and HNO_3. Before measurements, samples have been cleaned in acetone, isopropanol, methanol and DI water.

2.2. Fabrication of diamond nano-wires

Diamond nano-wires were produced via a top–down procedure using nickel particles as hard mask, as schematically shown in Fig. 1. A self-organised nickel particle array was prepared by firstly evaporating a thin Ni layer of 1 nm thickness onto diamond (Fig. 1a). For this purpose a Leybold A700 evaporation system was used. Then the nickel layer was annealed in vacuum at 700 °C for 5 min in an induction furnace. The heating and cooling ramp from room temperature to 700 °C takes 1 min and 30 min, respectively. Nickel particles of typically 10 nm to 30 nm in diameter were generated and distributed in a homogeneous pattern on the diamond surface (Fig. 1b). After formation of the Ni particle etching mask an oxygen inductive coupled plasma (ICP) is applied to etch diamond (Fig. 1c). Etching parameters were: oxygen gas flow 20 sccm, pressure 5×10^{-2} mbar, duration 5 min, power 1000 W. After the ICP process residual Ni particles are removed from the surface by wet-chemical cleaning in aqua-regia (Fig. 1d).

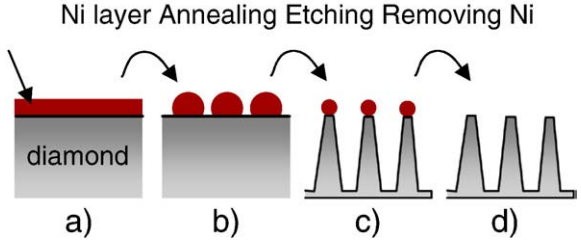

Fig. 1. Schematics of wire formation on diamond. (a) Evaporation of a thin Ni layer. (b) Annealing the sample at 700 °C for 5 min. (c) Etching diamond with oxygen ICP plasma. (d) Wet-chemical cleaning to remove Ni residua.

The length of nano-wires and the spacing in between can be controlled by the size of Ni particles and the etching time. Wire diameters of 10 nm to 60 nm can be realized. The lengths can be varied from a few nanometers to several microns, depending on the thickness of wires and the etching time.

2.3. Characterizations of diamond nano-wires

Nickel nano-particles and surface morphologies of diamond nano-wires were characterized by a Veeco Multi-mode Nanoscope V scanning probe microscope (CA, USA) and by a scanning electron microscopy (SEM: Zeiss 1540 ESB Gemini). Electrochemical experiments were conducted using a VMP-3 computer-controlled potentiostat (BioLogic Science Instruments, France) at room temperature with a conventional three-electrode configuration in a custom fabricated sample holder cell [16]. The exposed area to buffer solution was 0.053 cm^2. Background current of the diamond electrode was measured with cyclic voltammetry performed in 0.1 M KCl buffer solution. Redox activity was measured by adding 0.01 M $Fe(CN)_6^{3-/4-}$ in 0.1 M KCl.

3. Results and discussion

3.1. Formation of self-aligned Ni nano-particles

To characterize the effect of self assembly of nickel particles, morphologies of diamond surfaces were characterized before and after Ni evaporation and after thermal treatment of the sample. All of the AFM measurements show a low frequency background modulation which originates from polishing of diamond. Height profiles perpendicular to these height variations reveal a nano-scale roughness in the range of (2 to 4) nm. Before and after Ni evaporation no remarkable difference in surface roughness was observed indicating a homogeneous coverage of the diamonds surface with a closed nickel layer (AFM images not shown here).

Even though the melting point of nickel is at around 1450 °C, we observe a self-organised Ni nano-particle formation after annealing the sample at 700 °C for 5 min. The thin Ni layer is melting at temperatures significantly below the melting point of bulk material. This effect is referred as melting point lowering in the literature [35,36]. SEM and AFM images in Fig. 2a and b reveal dots with diameters of (17 ± 3) nm with a density of about $\sim10^{11}\,cm^{-2}$. A line scan profile of Ni nano-particles is shown in Fig. 2c (indicated by a blue line in Fig. 2b). With help of Fourier transformations and Gaussian fit calculations, the distance from dot to dot is obtained to be (40 ± 10) nm. Taking into account the thickness of the evaporated Ni layer of 1 nm, we have calculated the theoretical dimensions of a Ni particle that can be formed out of a $(40\times40\times1)\,nm^3$ Ni volume. Here we assumed a Ni particle shape of a hemisphere which yields typical Ni particle diameters of (20 ± 5) nm. This is in good agreement with AFM and SEM measurements.

3.2. Surface morphologies of diamond nano-wires

After ICP treatment the resulting diamond surface shows wires with typical diameters of (23 ± 7) nm (Fig. 3a). The density is about $10^{11}\,cm^{-2}$, which corresponds to the size and distribution of Ni particles. The height or length of wires is measured to be (1200 ± 200) nm (Fig. 3b,c) and the aspect ratio is in the range of 50. Calculations of the surface enlargement, assuming cylindrically shaped wires reveal a surface enlargement of 10 to 80. This is in good agreement with experimentally obtained data of the surface enlargement using capacitance-voltage measurements, which will be discussed below. Please note, that narrow standing diamond wires are cylindrical in

Please cite this article as: W. Smirnov, et al., Diam. Relat. Mater. (2009), doi:10.1016/j.diamond.2009.09.001

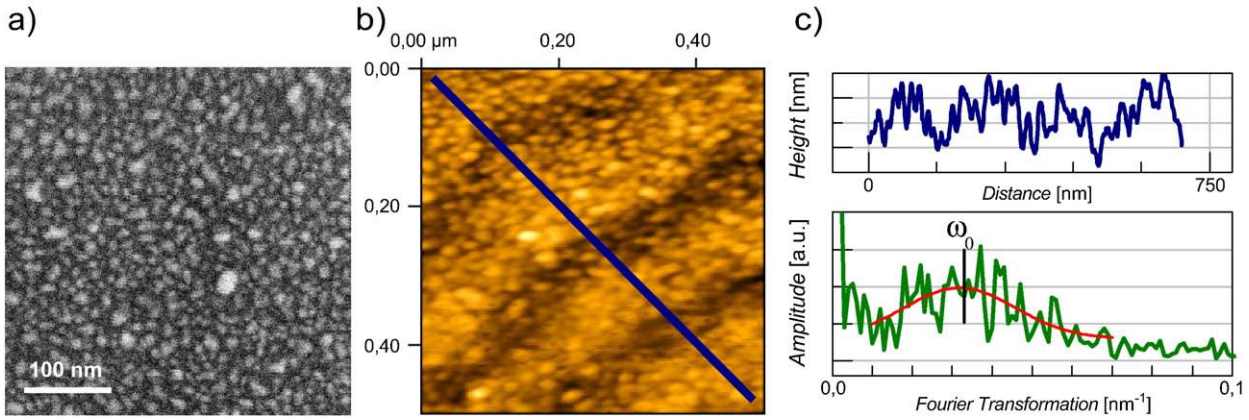

Fig. 2. Ni nano-particles examined by (a) SEM and (b) AFM. (c) Line scan as indicated by blue line in (b) and Fourier transformation with Gaussian fit revealing inverse particle to particle separation (indicated by ω_0). (For interpretation of the references to colour in this figure legend, the reader is referred to the web version of this article.)

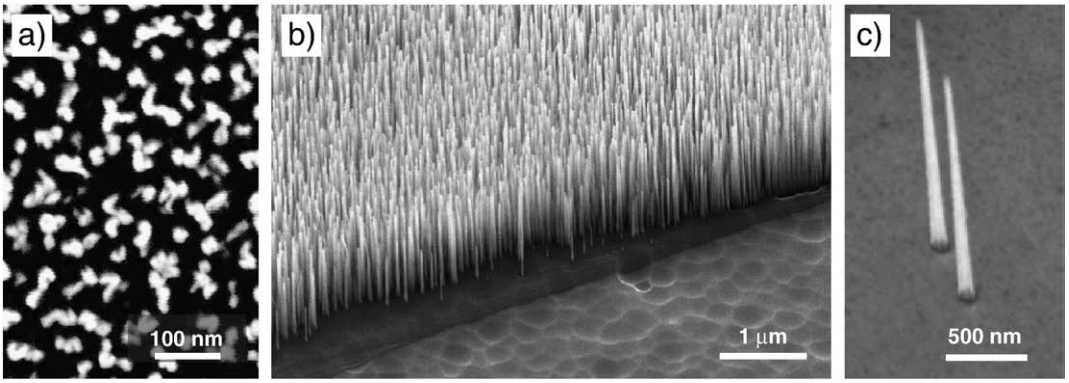

Fig. 3. SEM pictograms of diamond nano wires. (a) DNW array, view from top. (b) DNW array, taken at a 45° tilt angle with respect to sample surface. (c) Higher magnification of individual nano wires.

shape, whereas single, stand alone wires are conical in shape as can be seen in Fig. 3b and c. This effect may arise from plasma shielding during etching due to charging of the wires and reflected ions at wires [37].

3.3. Electrochemical characterizations

To detect the surface enlargement, we have applied cyclic voltammetry experiments on our structured electrodes. We compared samples obtained from the same diamond substrate — (i) without- and (ii) with nano-wires (s. Fig. 4). Dimensions of nano-wires were: height (1200 ± 200) nm, width (35 ± 5) nm, density ~10^{10} cm^{-2}.

In order to verify the surface enhancement of diamond nano-wires, the background currents were measured in 0.1 M KCl at a scan rate of $\nu = 50$ mV s^{-1}. The background current is proportional to the surface area in contact with the electrolyte solution and given by:

$$I_C = C_n \cdot A_{\text{Geom}} \cdot \nu \tag{1}$$

where I_c is the current related to the charging of the interfacial capacitance C_n given in units of (F/cm^{-2}) and A_{Geom} the total surface area. We assume that the capacitance per unit area is constant and not affected by the etching and formation of the wires as the diamond substrate has not been changed (boron doping is the same). We assume that the depletion layer width at the surface of diamond in buffer solution is therefore the same. This is, however, currently under investigation in our lab.

The background current on diamond nano-wires is more than 10 times larger than on the smooth diamond electrode. From this we can deduce, that the overall diamond surface is enhanced by a factor

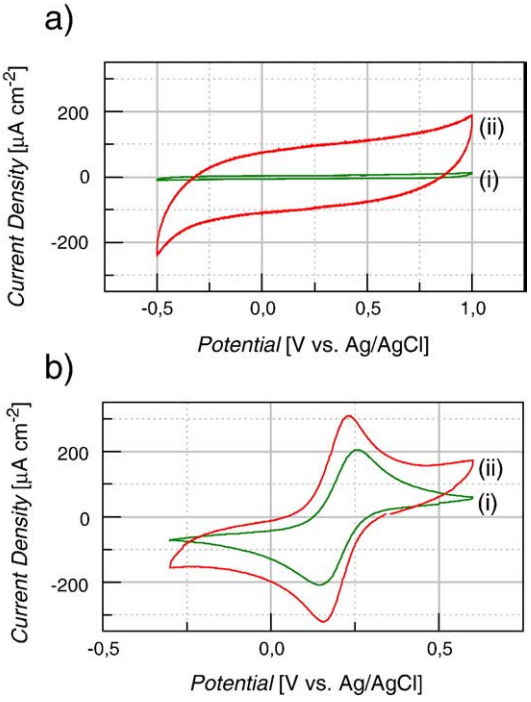

Fig. 4. Electrochemical experiments on i) smooth diamond surface and (ii) on diamond with nano wires: (a) Background currents as measured by cyclic voltammetry in 0.1 M KCl at a scan rate of 50 mV s^{-1} and (b) Redox currents as measured by cyclic voltammetry using 1 mM $Fe(CN)_6^{3-/4-}$ in 0.1 M KCl at a scan rate of 100 mV s^{-1}.

Please cite this article as: W. Smirnov, et al., Diam. Relat. Mater. (2009), doi:10.1016/j.diamond.2009.09.001

of 10 which is in agreement with geometrical calculation discussed previously.

The electrochemical activity of diamond nano-wires was characterized using redox couples of $Fe(CN)_6^{3-/4-}$ as probes. Fig. 4b shows cyclic voltammograms of 1.0 mM $Fe(CN)_6^{3-/4-}$ at a scan rate of $\nu = 100\,mV\,s^{-1}$. The peak splitting of oxidation and reduction currents (potential of the anodic peak minus potential of cathodic peak) is (80 ± 10) mV. It is close to the Nernst limit which is a result of metallically ultra-high doping. The enhancement in current density is, however, only 1.5. For a diffusion controlled process, the peak current (I_P) is proportional to the square root of the scan rate (ν), to the diffusion coefficient (D) and to the electrochemically active area ($A_{El\ Chem}$), as given by Eq. (2) [38]:

$$I_P \sim A_{El\ Chem} \cdot D^{1/2} \nu^{1/2} \quad (2)$$

For comparison of smooth diamond and diamond nano-wires we assume again that the only variable parameter is the area $A_{El\ Chem}$. Hence, the ratio of peak current slopes (I_p plotted against $\nu^{1/2}$, not shown here) can be used to calculate the surface enlargement which is only 1.5. This is much lower than the real increase of surface area. This is attributed to the following:

The capacitive background current in KCl is proportional to the total surface area in contact with electrolyte solution. On the other hand, the faradaic current of ferri/ferrocyanide is dominated by their diffusion length, L_D, which is typically in the range of tens of microns. Structures which are significantly smaller than L_D are not recognized and the faradaic current of ferri/ferrocyanide is therefore about the same as on a smooth surface. This diamond nano-wire electrode does not behave as a microelectrode ensemble but rather as a macro-electrode.

As a result, the electrochemically active area is significantly smaller than the total surface area. To evaluate the surface enlargement truly by this method requires redox molecules, which either drift in an electric field and/or which show a decreased electrochemical activity like hydrogen peroxide [39].

Wires for redox sensing therefore are promising as electrochemically selective detectors ("filter"). Such devices will be applied to distinguish between molecules of different, masses, charges, diffusion lengths and electron transfer properties.

4. Conclusions

In this paper we summarize and discuss how to produce homogeneously distributed vertically aligned diamond nano-wires with high aspect ratios above 50. These wires can be generated homogeneously either dense or dilute with long or short wires. Ni nano-particles are used which act as self-aligned and self-forming etching mask used in an ICP plasma (top–down approach). Ni particles are formed at 700 °C annealing temperature from a thin homogeneous Ni layer of 1 nm thickness, which is deposited on polished polycrystalline diamond substrates. After ICP etching using oxygen as etching gas we observe vertically aligned diamond wires with typical diameters of 20 nm and lengths up to 1000 nm. The diameter and distribution of wires is in agreement with the Ni nano-particle pattern generated by thermal annealing. The density of these wires is in the range of $10^{11}\,cm^{-2}$ and results in an effective surface enhancement of about 10 to 80, dependent on the length of the wires. Electrochemical analysis was used to characterize experimentally surface enlargements and electrochemical activity of wires. Electrochemical background current measurements reveal indeed a surface enhancement which is in agreement with calculations however the electrochemical activity of wires with respect to $Fe(CN)_6^{3-/4-}$ interaction is very little increasing.

This is attributed to the diffusion properties of $Fe(CN)_6^{3-/4-}$ in combination with the nano-spaced assembly of nano-wires.

Such a nano-structuring in combination with the unique electrochemical properties of diamond opens up a path to bio-electronic sensor applications with improvements in sensitivity, reproducibility and chemical stability required to meet future needs in various fields. Diamond nano-wires are very promising for future applications such as electrochemical filters, as spacer layer for bio-molecule on diamond surfaces or as super capacitors in battery application.

Acknowledgment

The authors would like to acknowledge the financial support from the Fraunhofer Attract program COMBIO — "Hybrid HF-MEMS Filters for GHz-Communication and capillary MEMS systems for chemical and bio-chemical sensing".

References

[1] M.J. Kim, J.S. Lee, S.K. Kim, G.Y. Yeom, J.-B. Yoo, C.-Y. Park, Thin Solid Films 475 (1–2) (2005) 41.
[2] T. Strother, W. Cai, X. Zhao, R.J. Hamers, Lloyd, M. Smith, J. Am. Chem. Soc. 122 (6) (2000) 1205.
[3] L. Gao, R.L. Woo, B. Liang, M. Pozuelo, S. Prikhodko, M. Jackson, N. Goel, M.K. Hudait, D.L. Huffaker, M.S. Goorsky, S. Kodambaka, R.F. Hicks, Nano Lett. 9 (6) (2009) 2223.
[4] K. Hashimoto, K. Ito, Y. Ishimori, Anal. Chem. 66 (21) (1994) 3830.
[5] F.J. Yusta, M.L. Hitchman, S.H. Shamlian, J. Mater. Chem. 7 (1997) 1421.
[6] H.-W. Huang, C.-C. Kao, T.-H. Hsueh, C.-C. Yu, C.-F. Lin, J.-T. Chu, H.-C. Kuo, S.-C. Wang, Mater. Sci. Eng. B 113 (2) (2004) 125.
[7] H.-W. Huang, C.-C. Kao, J.-T. Chu, W.-C. Wang, T.-C. Lu, H.-C. Kuo, S.-C. Wang, C.-C. Yu, S.-Y. Kuo, Mater. Sci. Eng. B 136 (2–3) (2007) 182.
[8] H. Kasugai, Y. Miyake, A. Honshio, S. Mishima, T. Kawashima, K. Iida, M. Iwaya, S. Kamiyama, H. Amano, I. Akasaki, H. Kinoshita, H. Shiomi, Jpn. J. Appl., Phys. 44 (2005) 7414.
[9] J. Wang, Electroanalysis 17 (1) (2004) 7.
[10] M.P. Anantram, F. Léonard, Rep. Prog. Phys. 69 (2006) 507.
[11] H. Miyagawa, M. Misra, A.K. Mohanty, J. Nanosci. Nanotechnol. 5 (10) (2005) 1593.
[12] J. Wilks, E. Wilks, Butterworth-Heinemann Limited, (1991).
[13] L. Ostrovskaya, V. Perevertailo, V. Ralchenko, A. Saveliev, V. Zhuravlev, Diam. Relat. Mater. 16 (12) (2007) 2109.
[14] N. Yang, H. Uetsuka, E. Osawa, C.E. Nebel, Angew. Chem. Int. Ed. 47 (28) (2008) 5183.
[15] O.A. Shenderova, C.W. Padgett, Z. Hu, D.W. Brenner, J. Vac. Sci. Technol., B 23 (2005) 2457.
[16] C.E. Nebel, B. Rezek, D. Shin, H. Uetsuka, N. Yang, J. Phys. D: Appl. Phys. 40 (2007) 6443.
[17] N. Yang, H. Uetsuka, E. Osawa, C.E. Nebel, Nano Lett. 8 (11) (2008) 3572.
[18] H. Uetsuka, T. Yamada, S. Shikata, Diamond Relat. Mater. 17 (4–5) (2008) 728.
[19] M.Y. Chen, Y.K. Chih, J. Hwang, C.S. Kou, M.T. Chang, L.J. Chou, Thin Solid Films 516 (21) (2008) 7595.
[20] E.-S. Baik, Y.-J. Baik, D. Jeon, Diamond Relat. Mater. 8 (12) (1999) 2169.
[21] M.-C. Kan, J.-L. Huang, J. Sung, K.-H. Chen, Thin Solid Films 447–448 (2004) 187.
[22] T. Yamada, D.S. Hwang, P.R. Vinod, T. Makino, N. Fujimori, Jpn. J. Appl. Phys. Part 2 — Lett. Express Lett. 44 (12–15) (2005) L385.
[23] L. Diederich, O.M. Küttel, P. Aebi, L. Schlapbach, Surf. Sci. 418 (1) (1998) 219.
[24] Q. Yang, W. Chen, C. Xiao, A. Hirose, R. Sammynaiken, Diamond Relat. Mater. 14 (10) (2005) 1683.
[25] Y.K. Chih, Y.L. Chueh, C.H. Chen, J. Hwang, L.J. Chou, C.S. Kou, Diamond Relat. Mater. 15 (9) (2006) 1246.
[26] M.L. Terranova, S. Orlanducci, A. Fiori, E. Tamburri, V. Sessa, M. Rossi, A.S. Barnard, Chem. Mater. 17 (12) (2005) 3214.
[27] D.S. Hwang, T. Saito, N. Fujimori, Diamond Relat. Mater. 13 (11–12) (2004) 2207.
[28] Y. Ando, Y. Nishibayashi, A. Sawabe, Diamond Relat. Mater. 13 (4–8) (2004) 633.
[29] C.Y. Li, A. Hatta, Diamond Relat. Mater. 15 (2–3) (2006) 357.
[30] E.-S. Baik, Y.-J. Baik, S.W. Lee, D. Jeon, Thin Solid Films 377–378 (2000) 295.
[31] Y.S. Zou, Y. Yang, W.J. Zhang, Y.M. Chong, B. He, I. Bello, S.T. Lee, Appl. Phys. Lett. 92 (2008) 053105.
[32] O. Babchenko, A. Kromka, K. Hruska, M. Michalka, J. Potmesil, M. Vanecek, Cent. Eur. J. Phys. 7 (2) (2009) 310.
[33] M. Füner, C. Wild, P. Koidl, Appl. Phys. Lett. 72 (1998) 1149.
[34] H.O. Finklea, in: H.O. Finklea (Ed.), Semiconductor Electrodes, Elsevier, Amsterdam, 1988, p. 27.
[35] P.R. Couchman, W.A. Jesser, Nature 269 (5628) (1977) 481.
[36] P. Buffat, J.P. Borel, Phys. Rev. A 13 (6) (1976) 2287.
[37] I.W. Rangelow, Deep Etching Of Silicon, Oficyna Wydawnicza Politechniki Wroclawskiej, Wroclaw, 1996.
[38] J. Wang, Analytical Electrochemistry, second ed.Wiley-VCH, New Jersey, 2000.
[39] S.M. Macdonald, K. Szot, J. Niedziolka, F. Marken, M. Opallo, J. Solid State Electrochem. 12 (3) (2008) 287.

Please cite this article as: W. Smirnov, et al., Diam. Relat. Mater. (2009), doi:10.1016/j.diamond.2009.09.001